NASA TN D-188

TECHNICAL NOTE

D-188

STATIC STABILITY AND SEPARATION CHARACTERISTICS OF A TWO-STAGE ROCKET CONFIGURATION AT MACH NUMBERS FROM 1.57 TO 4.50

By Kenneth L. Turner, David S. Shaw, and Laurence W. Enderson, Jr.

Langley Research Center
Langley Field, Va.

NATIONAL AERONAUTICS AND SPACE ADMINISTRATION

WASHINGTON

January 1960

NATIONAL AERONAUTICS AND SPACE ADMINISTRATION

TECHNICAL NOTE D-188

STATIC STABILITY AND SEPARATION CHARACTERISTICS OF A TWO-STAGE ROCKET CONFIGURATION AT MACH NUMBERS FROM 1.57 TO 4.50

By Kenneth L. Turner, David S. Shaw,
and Laurence W. Enderson, Jr.

SUMMARY

An investigation to determine the static stability and separation characteristics of a two-stage rocket configuration has been conducted in the Langley Unitary Plan wind tunnel. Each stage is a body of revolution with length-diameter ratio of approximately 8. The stages were tested separately, combined, and during systematic separation from each other. This paper contains axial force, static stability, and separation characteristics obtained at Mach numbers from 1.57 to 4.50 and Reynolds numbers per foot of approximately 1.5×10^6 to 4.0×10^6.

Results show that the complete model is statically stable throughout the test Mach number range. To insure a successful separation of the two stages, it appears that stage II should be ignited before separation or that auxiliary devices (such as retrograde rockets on stage I) should be employed to separate the two stages.

INTRODUCTION

It is well known that staging is a necessary requirement in obtaining high-performance rocket-vehicle systems. However, before such a vehicle can be made operational, many factors must be investigated. Among these are the separation characteristics of the stages and the aerodynamic characteristics of the entire vehicle and its separate components.

The National Aeronautics and Space Administration has designed a high-energy liquid-fuel rocket engine and, for development purposes, a vehicle in which to house this engine. For the tests presented herein, this vehicle is used as the second stage of a two-stage rocket configuration. The aerodynamic characteristics of each configuration must be obtained in order to determine whether any corrective measures are necessary to insure positive stability of each configuration throughout the Mach number range. The separation characteristics should also be obtained in order to determine whether auxiliary separation devices are necessary.

The Langley Unitary Plan wind tunnel has, therefore, undertaken wind-tunnel tests to determine the aerodynamic characteristics of this two-stage configuration as well as the axial-force characteristics of both stages during separation. Also determined were aerodynamic characteristics of each stage after separation.

The tests were performed at Mach numbers that varied from 1.57 to 4.50, and the Reynolds number per foot ranged from about 1.5×10^6 to 4.0×10^6.

SYMBOLS

The coefficients of forces and moments are referred to the body-axis system (fig. 1). All aerodynamic moments were taken about the center of gravity of each specific test configuration (fig. 2). The symbols used in this paper are as follows:

C_A axial-force coefficient, $\frac{\text{Axial force}}{qS}$

$C_{A,b}$ base axial-force coefficient, $\frac{\text{Base axial force}}{qS}$

C_m pitching-moment coefficient, $\frac{\text{Pitching moment}}{qSd}$

C_{m_α} slope of pitching-moment-coefficient curve

C_N normal-force coefficient, $\frac{\text{Normal force}}{qS}$

C_{N_α} slope of normal-force-coefficient curve

d	missile diameter (2.125 in. for stage I and the complete configuration; 2.210 in. for stage II)
p_t	tunnel stagnation pressure, lb/sq in. abs
M	free-stream Mach number
q	free-stream dynamic pressure, lb/sq ft
R	Reynolds number per foot
S	cross-sectional area of the cylindrical body, sq ft
T_t	stagnation temperature, $^{\circ}F$
x_{cp}	distance from base of stage I to center of pressure of complete configuration, in.
$\frac{x_s}{d_2}$	ratio of separation distance between nose of stage I and base of stage II to stage II body diameter (2.210 in.)
α	angle of attack of body center line, deg
ϕ	model roll angle, deg ($\phi = 0^{\circ}$ when auxiliary rockets and conduits are horizontal; $\phi = 90^{\circ}$ when auxiliary rockets and conduits are vertical)

APPARATUS AND TESTS

Tunnel

The tests were performed in both the low and high Mach number test sections of the Langley Unitary Plan wind tunnel, which is a variable-pressure continuous-flow tunnel. Each test section is approximately 4 feet square and 7 feet long. The nozzle leading to each test section is of the asymmetric sliding-block type, which permits a continuous variation of Mach number from approximately 1.5 to 2.9 in the low Mach number test section and from approximately 2.3 to 4.7 in the high Mach number test section.

Model Support System

For the tests of the separate stages and complete configuration the models were mounted on a six-component internal strain-gage balance

which, in turn, was supported by a sting. For the separation tests, stage I was mounted on the six-component balance and stage II was mounted on a translating strut (fig. 2) which was remotely operated during the separation of these stages. Since the translating strut afforded values of x_s/d_2 only up to 2.72, and it was desired to obtain data at values of x_s/d_2 up to about 4.8, it was necessary to attach the strut to the stage II model at two separate locations. A photograph of the separation configuration is presented as figure 3(b).

Models

The models were constructed of wood and plastic. Photographs of the models are presented as figure 3. Drawings of the models are presented as figure 2. Stage I and stage II were bodies of revolution with length-diameter ratios of approximately 8. Two auxiliary rocket models were added to the rear portion of stage I. These rockets were 180° apart and were interdigitated with a set of wedge-section cruciform fins. Two sizes of fins were tested on stage I. However, unless otherwise noted, the smaller fins were being used.

Stage II had a 6° flared afterbody to which wedge-section cruciform fins were added, in line with the fins of stage I. Two conduits were also added to stage II, 180° apart and in line with the auxiliary rockets of stage I.

Test Conditions

The tests were performed through an angle-of-attack range of approximately -4° to 7° at Mach numbers from 1.57 to 4.50. The test configurations included stage I and stage II in combination (incorporating two different fin sizes on stage I), the separation of stage I from stage II, stage I alone, and stage II alone. The tests of the complete configuration and stage II alone at a Mach number of 4.50 were performed at two Reynolds numbers.

The separation tests and the tests of stage I and stage II alone were performed at a Mach number of 4.50 only, because the separation of the two stages of this particular configuration is to take place at this Mach number. The results obtained are for a power-off condition.

The dewpoint was maintained below -30° F for all Mach numbers in order to assure negligible condensation effects. Tests were performed at the following conditions:

Model	M	T_t, °F	p_t, lb/sq in. abs	R, per ft	Test range
Stage I and stage II combination	1.57	125	8	2.2×10^6	$\alpha = -4^\circ$ to 7°
	2.06	125	11	2.5	$\alpha = -4^\circ$ to 7°
			20	3.8	$\alpha = -4^\circ$ to 7°
	2.30	150	8	1.5	$\alpha = -4^\circ$ to 7°
	3.50	150	40	4.0	$\alpha = -4^\circ$ to 7°
	4.50	150	28	1.6	$\alpha = -4^\circ$ to 7°
			70	4.0	
Stage I and stage II separation	4.50	175	28	1.6×10^6	$x_s/d_2 = 0.45$ to 4.86
Stage I	4.50	175	28	1.6×10^6	$\alpha = -4^\circ$ to 7°
Stage II	4.50	175	70	4.0×10^6	$\alpha = -4^\circ$ to 7°
			28	1.6	

To assure turbulent flow over the model, a transition strip was fixed around the nose of the stage II model 1 inch from the forward end. The transition strip was 1/8 inch wide and consisted of No. 60 carborundum grains (nominal height of 0.012 inch) embedded in shellac. Experience has shown that transition strips of this size are sufficient to produce turbulent flow over the model at the test Reynolds numbers and Mach numbers. Because of the nose shape of stage I it was felt that artificially fixed transition for this component was unnecessary.

Corrections

The angles of attack have been corrected for tunnel-flow angularity and deflection of the balance and sting under aerodynamic loads. The axial-force data have been adjusted to correspond to zero base axial-force coefficient ($C_{A,b} = 0$). Examples of the variation of measured base axial force on stage I and stage II are presented in figures 4 and 5.

Accuracy

The accuracy of the individual measured quantities, based on calibration and repeatability of data, is estimated to be within the following limits:

R	C_N	C_A	C_m	M	x_s/d_2, in.	α, deg
4.0×10^6	±0.075	±0.003	±0.085	±0.015	±0.010	±0.100
3.8	±.045	±.002	±.049	±.015	±.010	±.100
2.5	±.070	±.003	±.078	±.015	±.010	±.100
2.2	±.075	±.003	±.080	±.015	±.010	±.100
1.6, 1.5	±.200	±.006	±.360	±.015	±.010	±.100

L 4 7 2

PRESENTATION OF RESULTS

DISCUSSION

Complete Configuration

It would be expected that for the complete configuration, the curves for the variation of normal-force coefficient and pitching-moment coefficient with angle of attack would go through zero. However, it may be seen in figure 9 that there is an offset in C_N and C_m at zero angle of attack. These offsets are believed to be due to slight misalinements of the model.

It may also be seen in figure 9 that the complete configuration is stable throughout the test Mach number range, and that both C_{m_α} and C_{N_α} decrease with an increase in Mach number. Figure 11 shows the estimated center-of-gravity travel due to fuel consumption, plotted against Mach number under the assumption of a linear variation of the center of gravity with Mach number. The base of stage I was taken as the zero ordinate, the distance being measured toward the nose.

This figure also shows the center-of-pressure locations at each Mach number of the investigation as obtained from the data shown in figures 9 and 10 for both the small and the large fins. The center-of-pressure values were obtained from the slopes of the pitching-moment-coefficient and normal-force-coefficient curves near zero angle of attack. It may be seen that the static margin available at a Mach number of about 3 is very small, and the slightly larger fins increase the static margin considerably. The center-of-gravity travel plotted in figure 11 is approximate, and a small difference between the values plotted and the center-of-gravity travel of the full-scale missile near a Mach number of 3 could cause the missile with the small fins to become unstable. The complete configuration, therefore, should probably incorporate the large fins to insure a positive static margin throughout the Mach number range of the tests.

From figure 12 it may be seen that the complete configuration at a roll angle of 90° is more stable and produces a greater normal-force slope than at a roll angle of 0°, a result which would not be expected from a consideration of the model geometry. This effect is believed to be due to a flow interference caused by the auxiliary rockets. When the model is rotated from 0° to 90°, this flow interference changes in such a way as to cause an increase in normal force on the fins of stage I, and, therefore, an increase in stability. The effect of Mach number variation on the stability and normal-force parameters of the complete configuration at model roll angles of 0° and 90°, as well as the complete configuration with small and large fins, is summarized in figure 14.

Stage I

Stage I (alone) was tested only at a Mach number of 4.50 and a Reynolds number of 1.6×10^6 since the missile is to separate at this Mach number. The model roll angle was 0°. At these test conditions, stage I was slightly stable and produced a positive normal-force slope (fig. 13). The derivatives C_{m_α} and C_{N_α} for stage I alone at a Mach number of 4.5 are also included in figure 14.

Stage II

Stage II (alone) also was tested only at a Mach number of 4.50; however, these tests were performed at a Reynolds number per foot of 4.0×10^6 as well as 1.6×10^6. From figure 15 it may be seen that this amount of change in Reynolds number had little or no effect upon the pitching-moment coefficients and the normal-force coefficients at angles of attack from -2° to 5°; however, the increase in Reynolds number caused a decrease in the axial-force coefficients, as might be expected because of the reduction in skin friction associated with an increase in Reynolds number. This figure also shows that stage II was stable and produced a positive slope of the normal-force curves at both Reynolds numbers. The derivatives C_{m_α} and C_{N_α} of stage II at a Mach number of 4.50 are also presented in figure 14.

Separation

The separation tests, as previously mentioned, were performed at a Mach number of 4.50. The model roll angle was 0°. Tests were conducted at $\alpha = 0.9^\circ$ and $\alpha = 1.9^\circ$ to determine the effect of a small change in angle of attack on the separation characteristics. During the separation tests, stage II was instrumented to measure only base pressure. The axial-force coefficients for stage II during separation were determined by assuming a constant forebody drag and adjusting the axial-force data obtained to correspond to the separation base pressure. These data are presented in figure 16 along with the data from stage I, which housed the balance. Axial force was the only component of stage II that could be determined during separation. It is believed that the strut supporting stage II had very little effect on the axial force of stage I during the separation. Unpublished data from a previous test in which a similar strut was used substantiates this belief.

It may be noted from figure 16 that the pitching-moment coefficients and normal-force coefficients of stage I were erratic. This is believed to be due to a change in the flow field acting on stage I as

the separation distance x_s/d_2 changes. It is also seen in figure 16 that the axial-force coefficient of stage I changes slightly with changes in x_s/d_2 up to an x_s/d_2 value of about 3.2, at which point the axial-force coefficients increase rapidly with further increase in separation distance. This result may be explained by observing the schlieren photographs of figure 7, which show the flow pattern during separation. At x_s/d_2 distances greater than about 3.16 the wake behind stage II begins to close and allow high-energy air to impinge on the face of stage I, thus causing the large increase in axial force experienced by stage I.

The axial-force coefficients of stage II during separation are also shown in figure 16. It may be seen that there is only a slight variation in these coefficients during separation. The axial-force coefficients of stage I are seen to be only slightly greater than those of stage II up to an x_s/d_2 value of about 3.2. At x_s/d_2 values greater than 3.2 the axial-force coefficients of stage I are much larger than those of stage II. To insure a successful separation of the two stages, it appears that stage II should fire before separation or that auxiliary devices (such as retrograde rockets on stage I) should be employed to separate the two stages up to a distance x_s/d_2 of about 3.2. At distances greater than this the two stages should separate because of the axial-force difference between these two stages. The separation is contingent not only on the drag of each stage, but also on the mass of stage I being less than that of stage II, a condition which would be expected since separation would take place after the fuel of stage I was expended. The interference-free values of the coefficients are included on the right side of figure 16 for comparison purposes.

CONCLUSIONS

The results of a static-stability and separation investigation of a model of a two-stage rocket at Mach numbers from 1.57 to 4.50 and Reynolds numbers per foot from 1.5×10^6 to 4.0×10^6 indicate the following conclusions:

1. The complete configuration is statically stable throughout the test Mach number range. The stability and normal-force parameters decrease with an increase in Mach number.

2. The complete configuration should incorporate the larger fins to insure a positive static margin throughout the Mach number range of the test.

3. The complete configuration at a model roll angle of 90° is more stable and produces more normal force than at a model roll angle of 0°.

4. Stage II is stable and produces positive normal force at a Mach number of 4.50.

5. To insure a successful separation of the two stages it appears that stage II should be ignited before separation or that auxiliary devices (such as retrograde rockets on stage I) should be employed to separate the two stages up to approximately 3.5 body diameters of stage II.

Langley Research Center,
National Aeronautics and Space Administration,
Langley Field, Va., August 20, 1959.

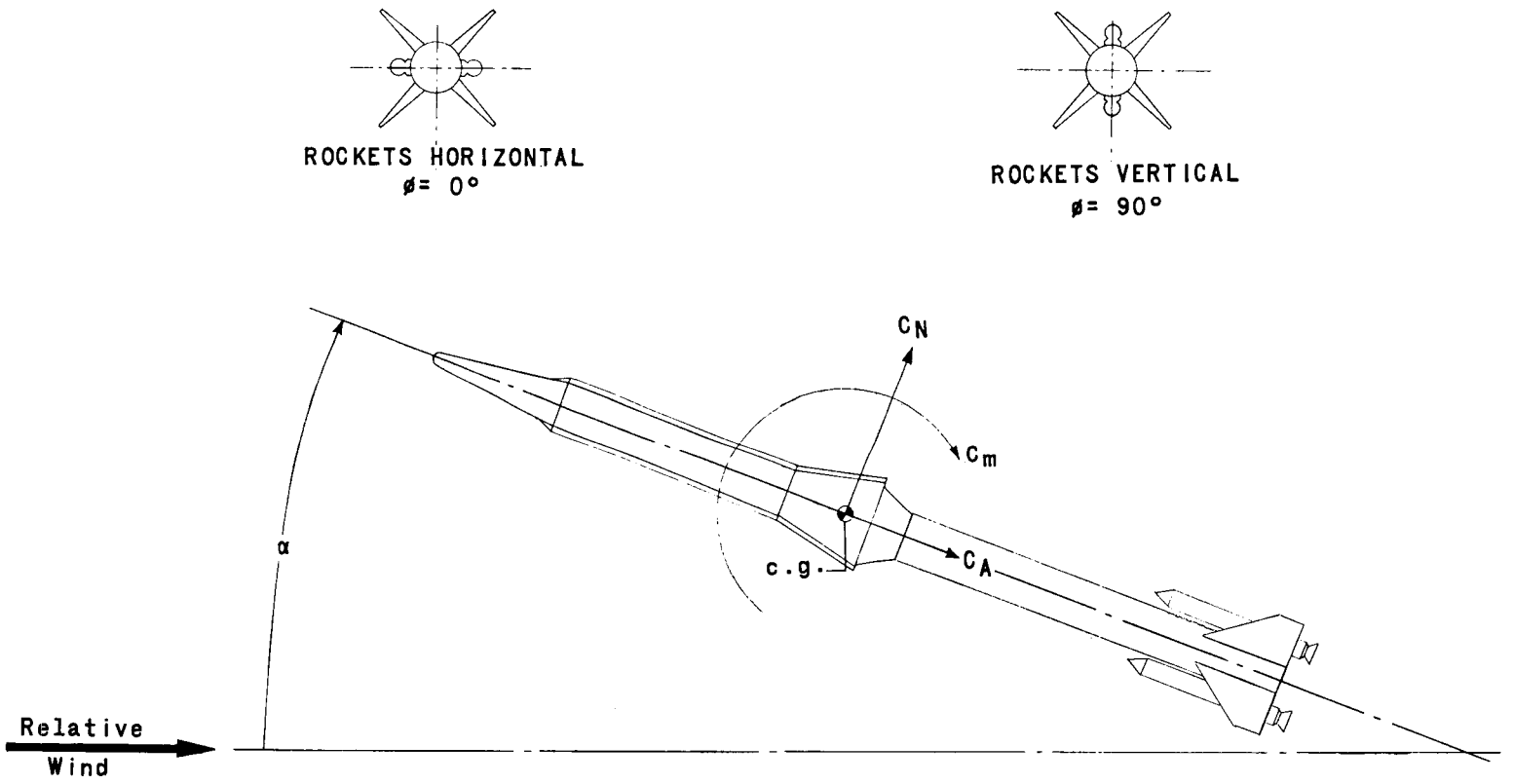

Figure 1.- Body-axis system. (Arrows indicate positive direction.)

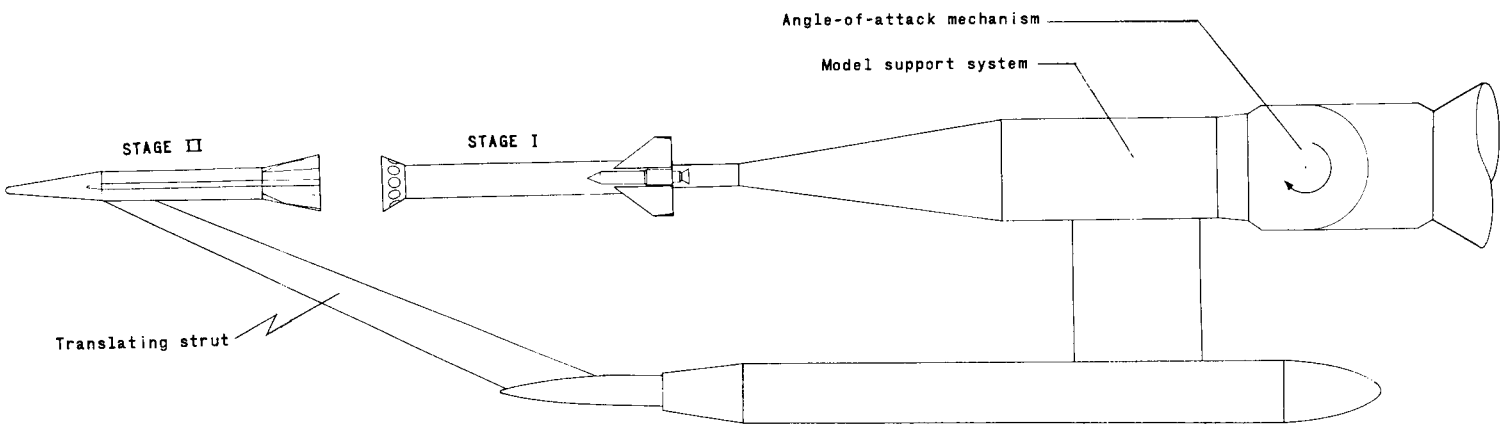

(a) Support system.

Figure 2.- Models and support system.

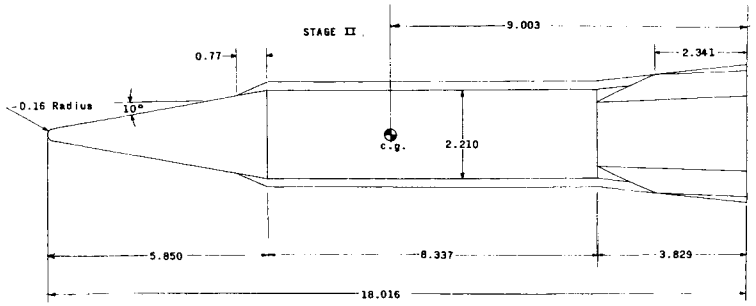

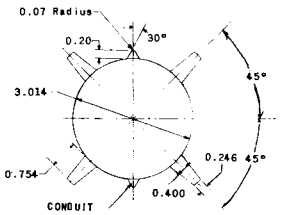

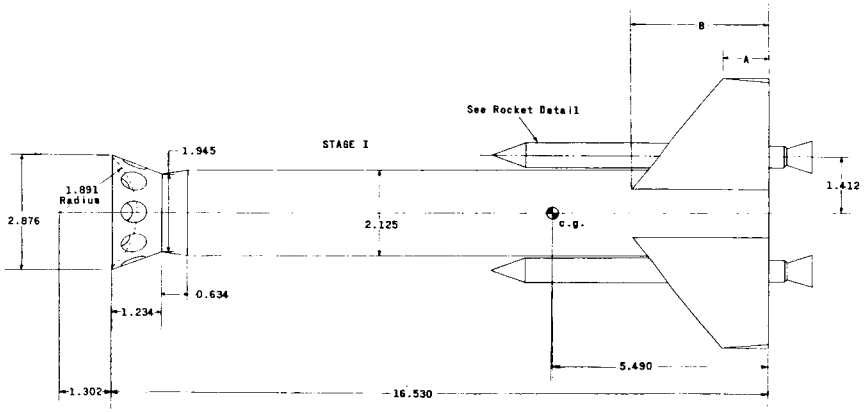

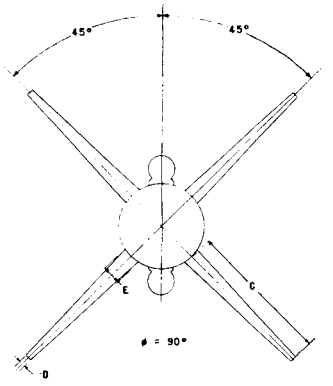

FIN DIMENSIONS

Fin Size	Area, in^2	A	B	C	D	E
Small	8.135	1.140	3.363	3.613	0.158	0.468
Large	9.487	1.230	3.630	3.904	0.246	0.506

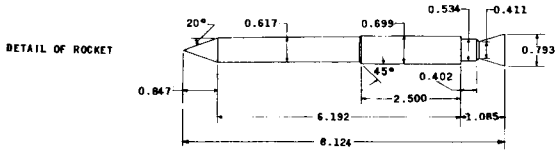

(b) Dimensions of models.

Figure 2.- Continued.

Complete Configuration

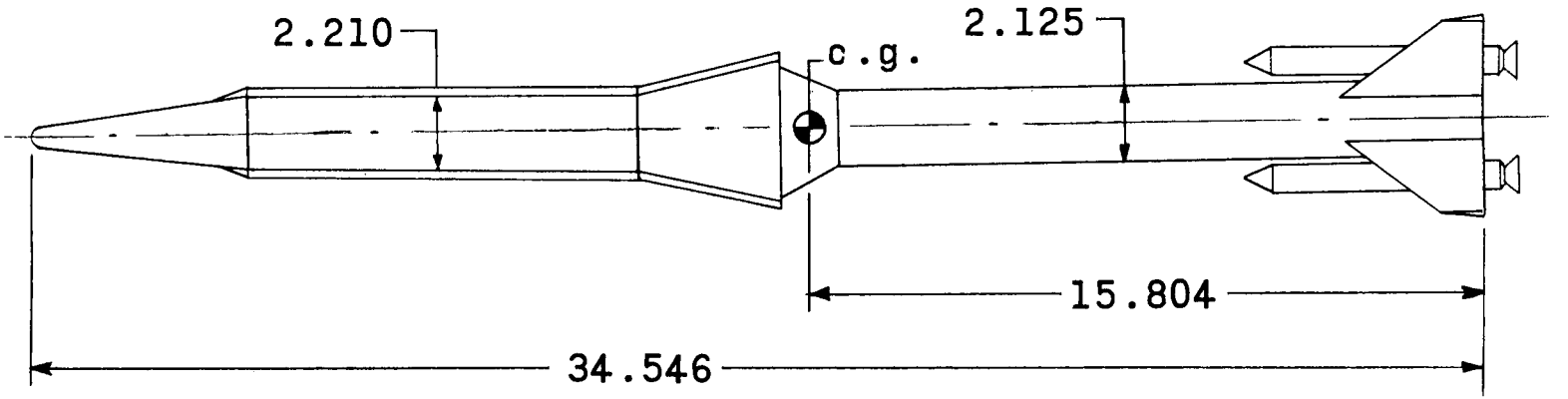

(b) Concluded.

Figure 2.- Concluded.

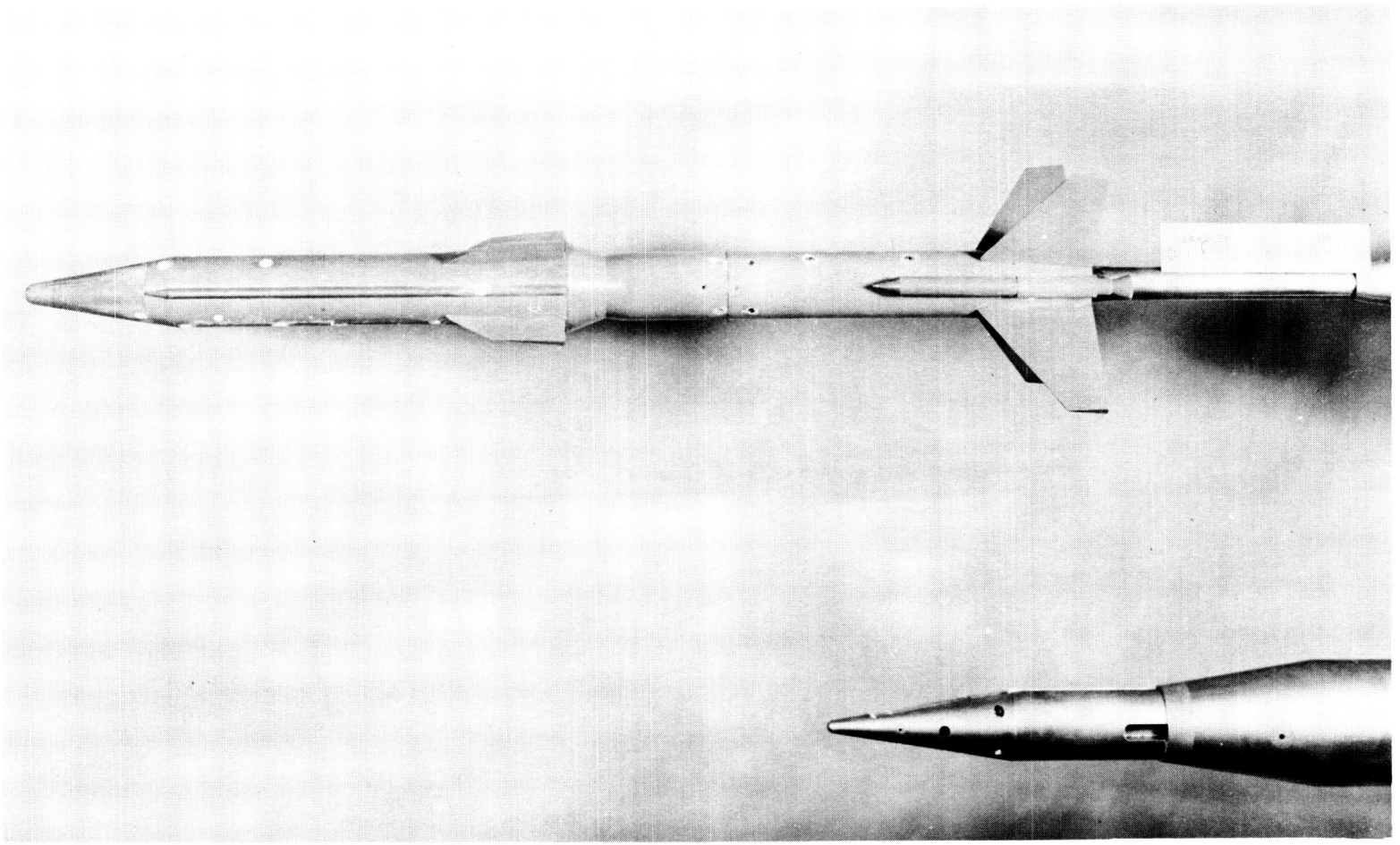

(a) Complete configuration. $\phi = 0^{\circ}$. L-58-669a

Figure 3.- Photographs of configurations.

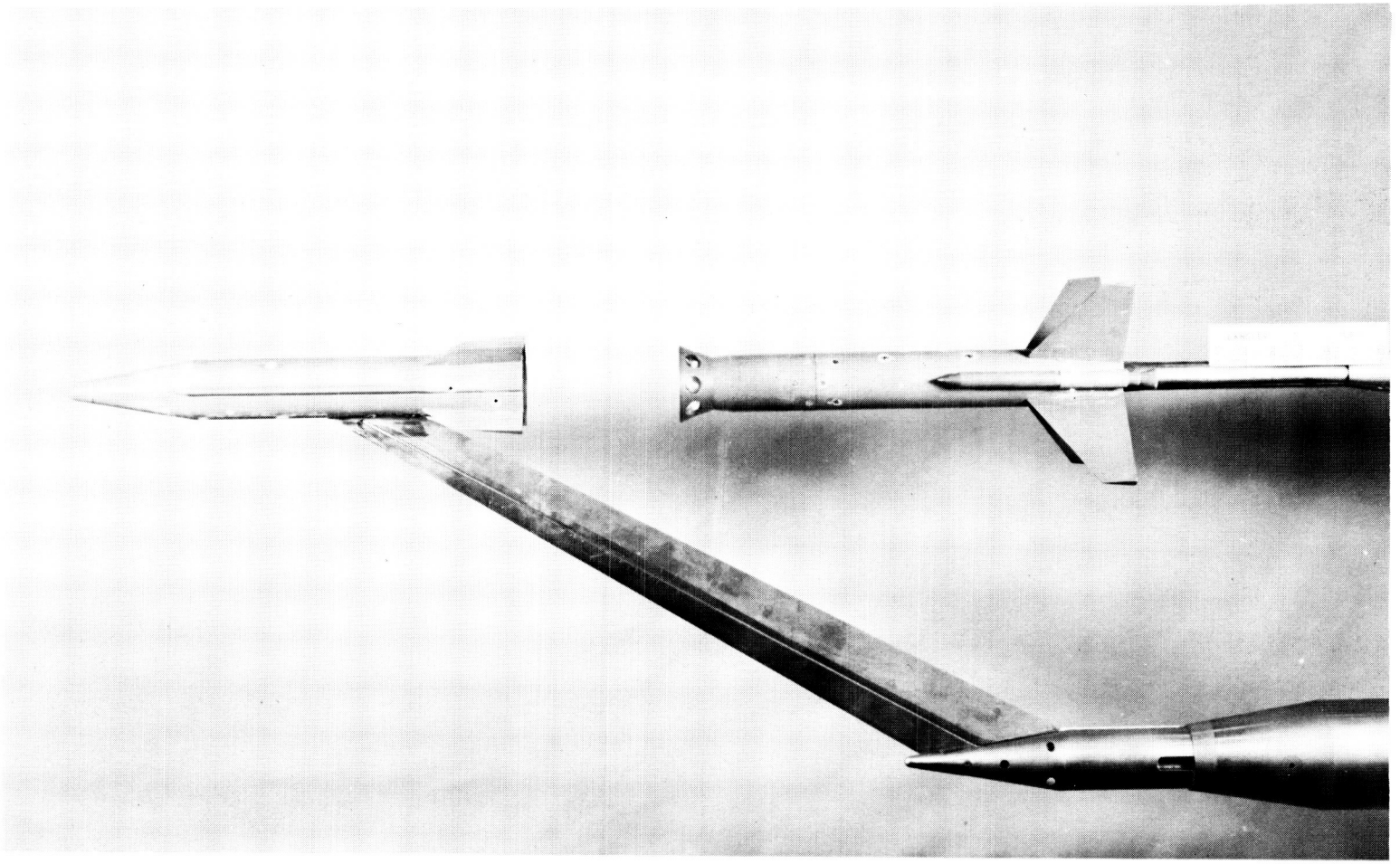

(b) Separation configuration. $\phi = 0^{\circ}$. L-58-668a

Figure 3.- Continued.

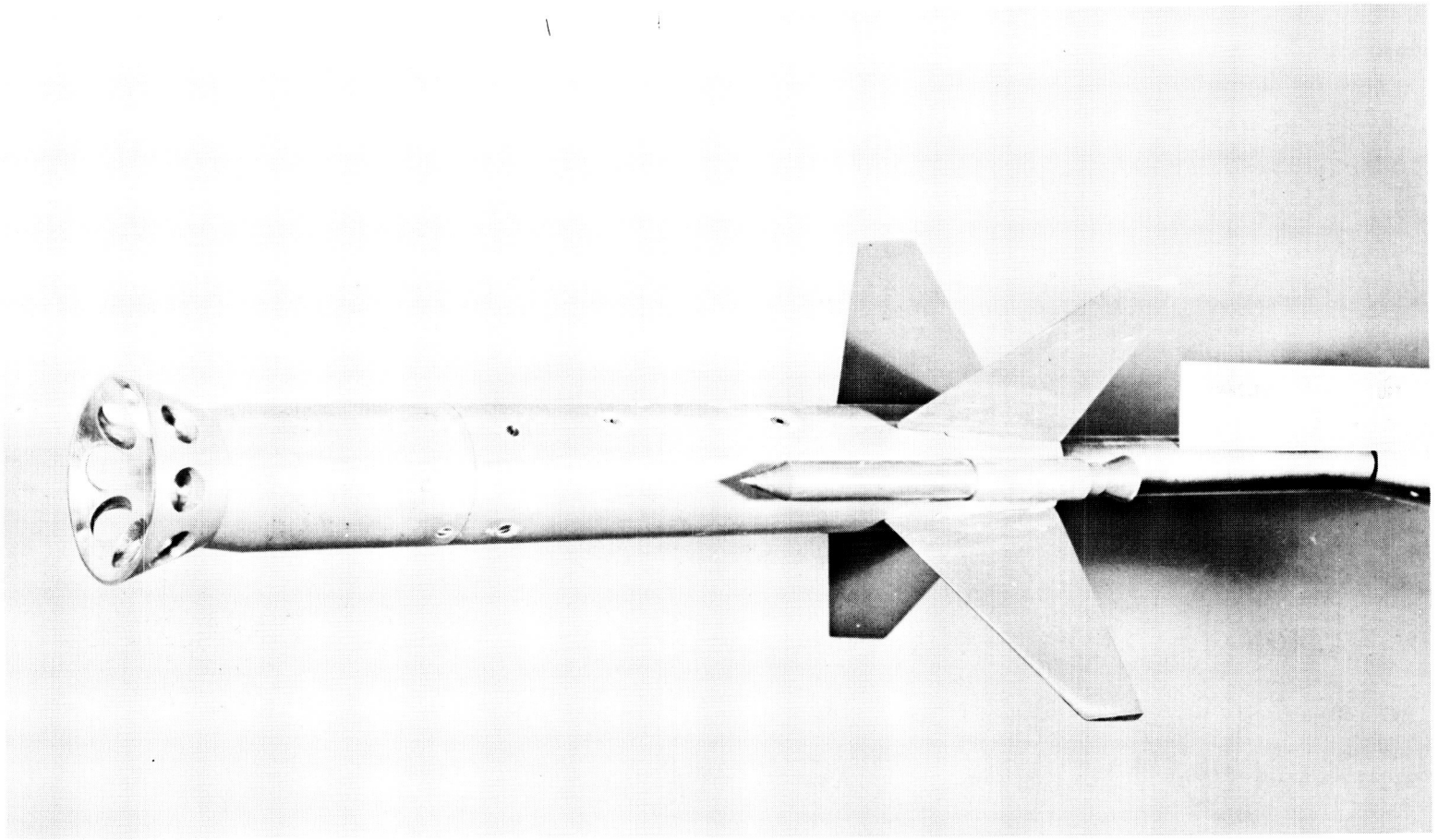

(c) Stage I. $\phi = 0^{\circ}$. L-58-670a

Figure 3.- Continued.

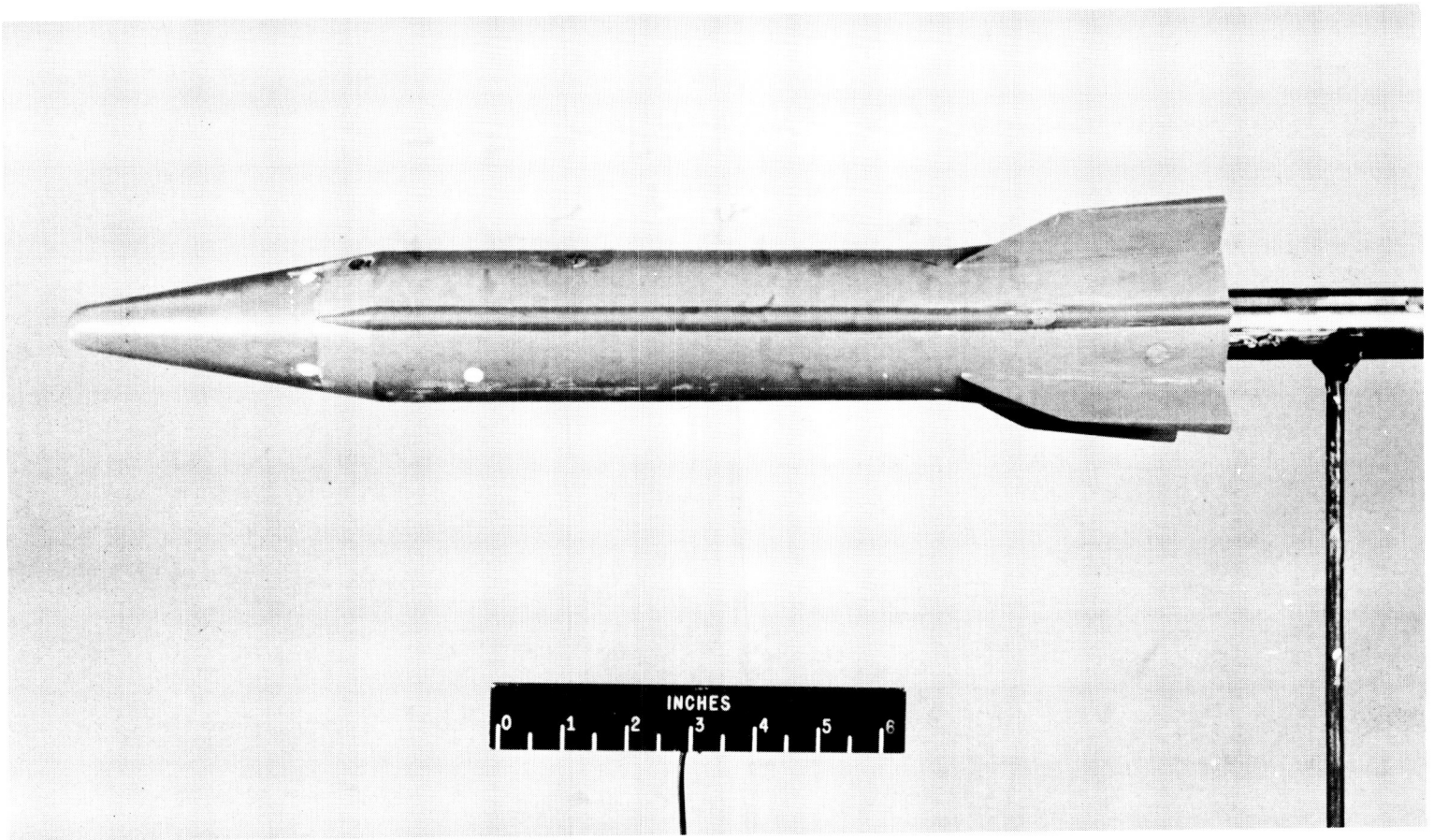

(d) Stage II. $\phi = 0^{\circ}$. L-59-314

Figure 3.- Concluded.

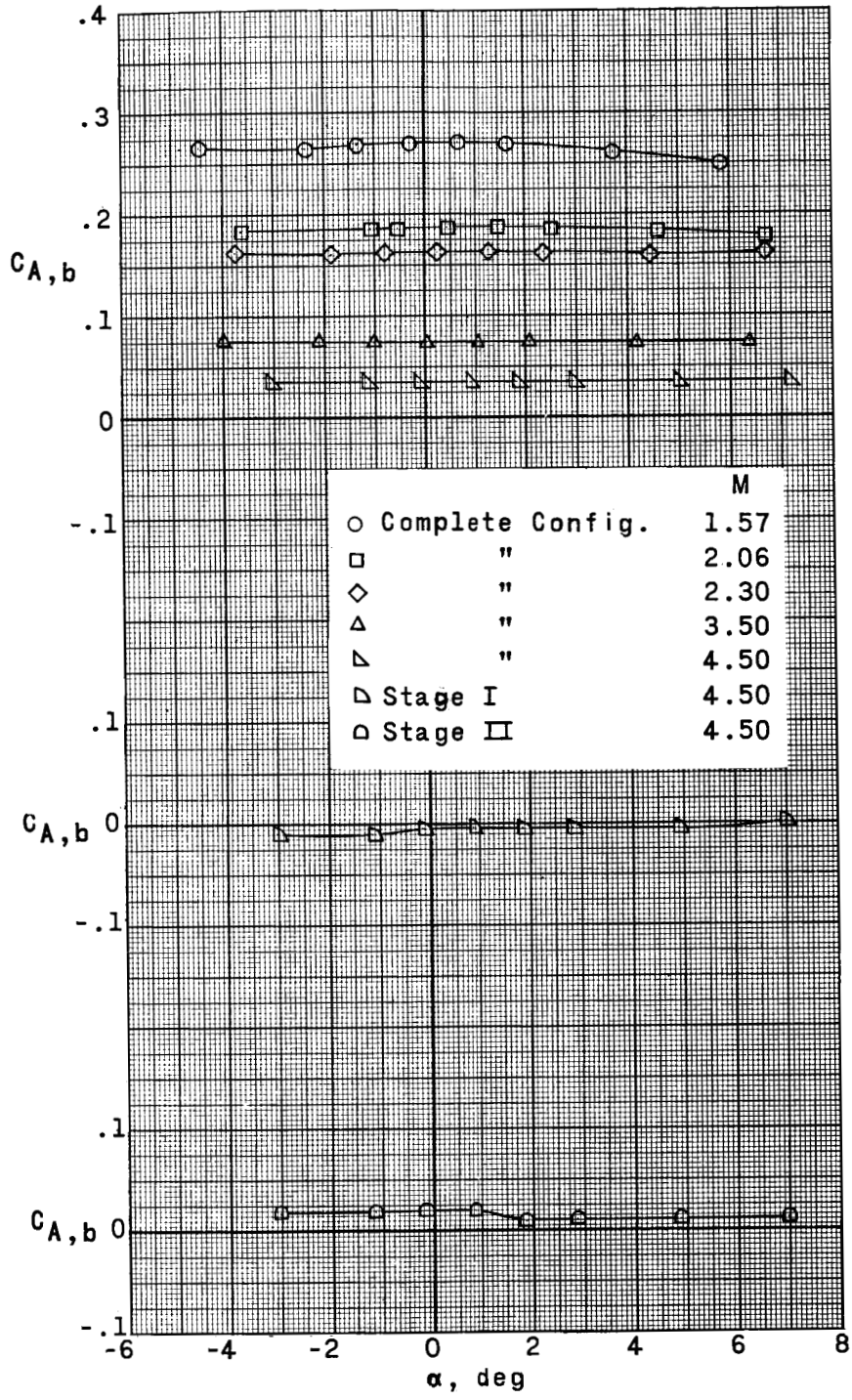

Figure 4.- Base axial-force coefficients of stage I, stage II, and complete configuration in pitch. $\phi = 0^{\circ}$.

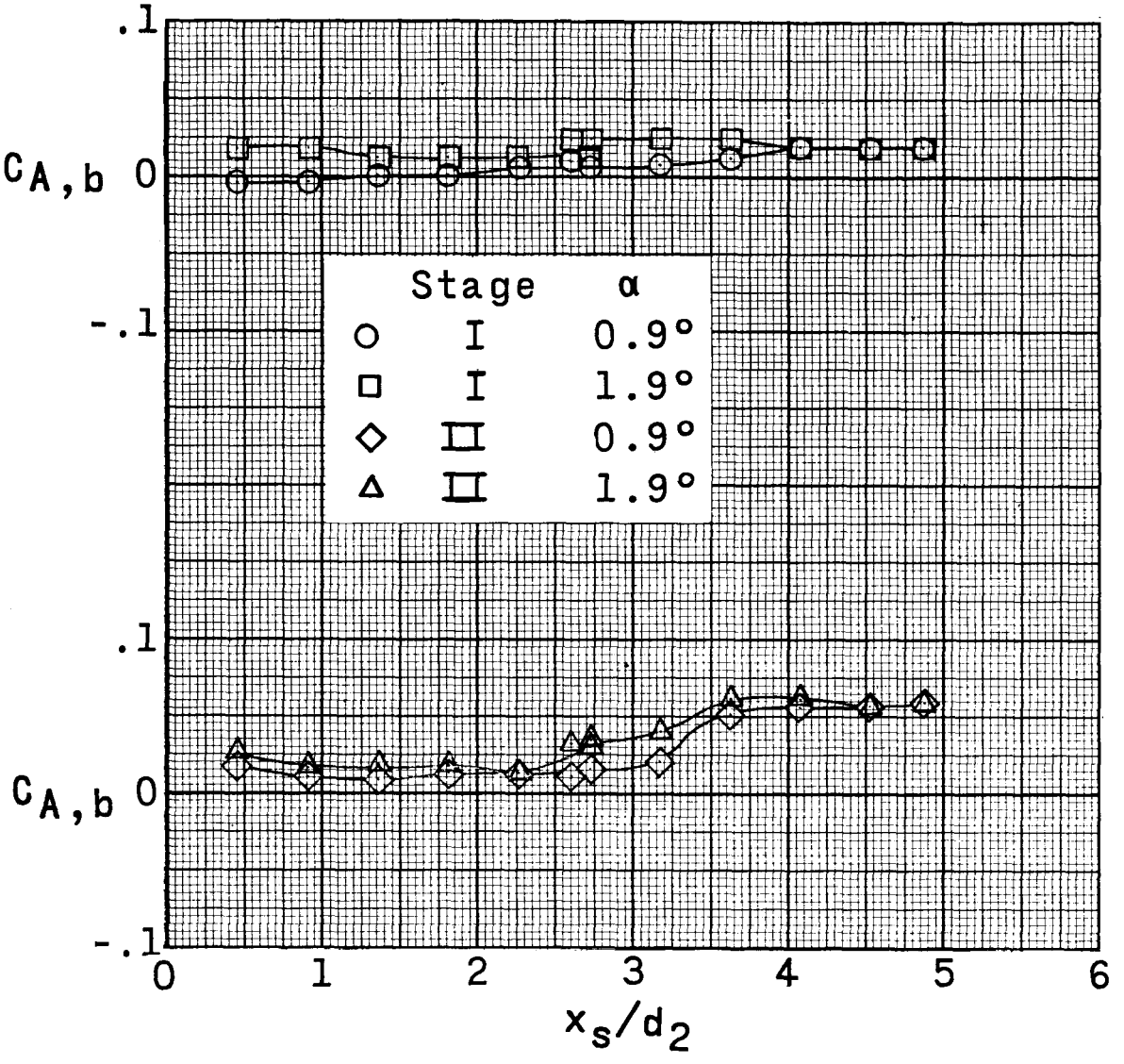

Figure 5.- Base axial-force coefficients of stage I and stage II during separation. $M = 4.50$; $R = 1.6 \times 10^6$; $\phi = 0^\circ$.

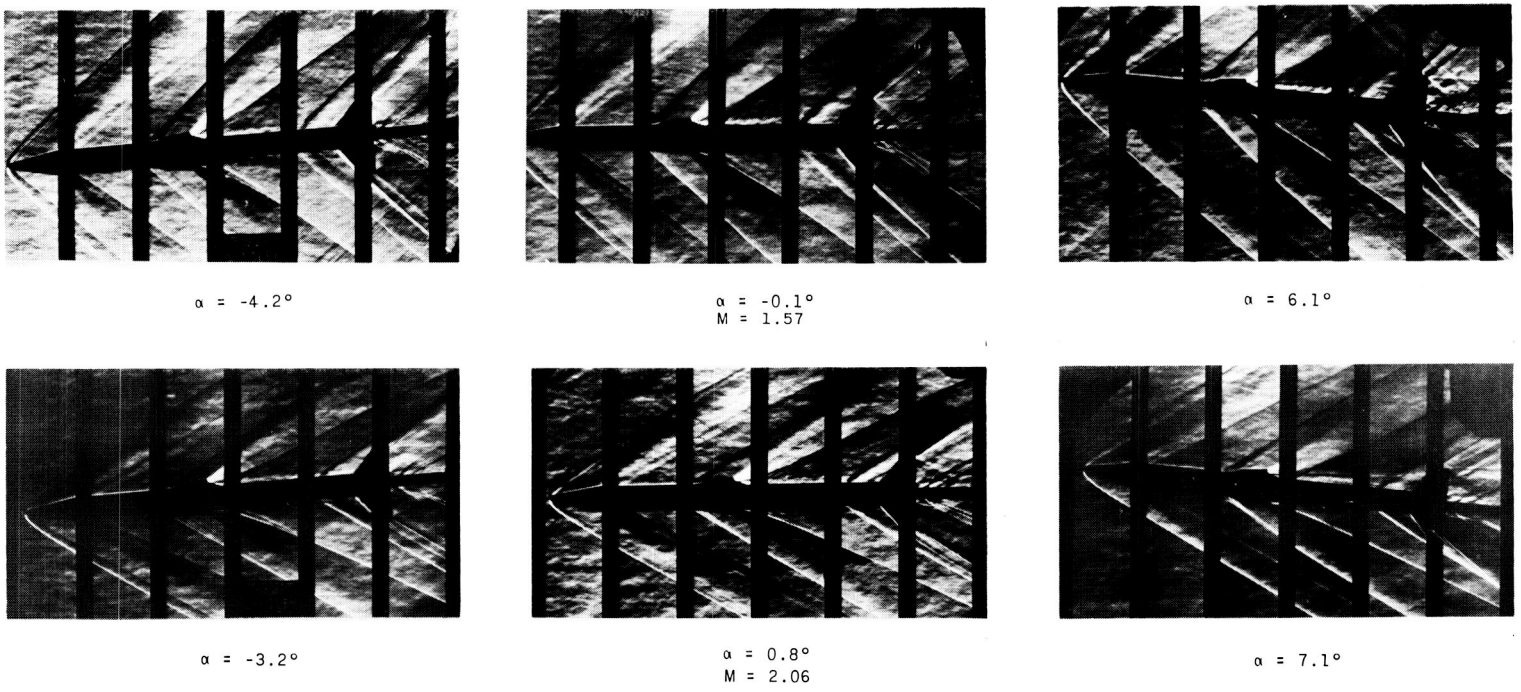

(a) $\phi = 0^{\circ}$.

L-59-6036

Figure 6.- Schlieren photographs of complete configuration.

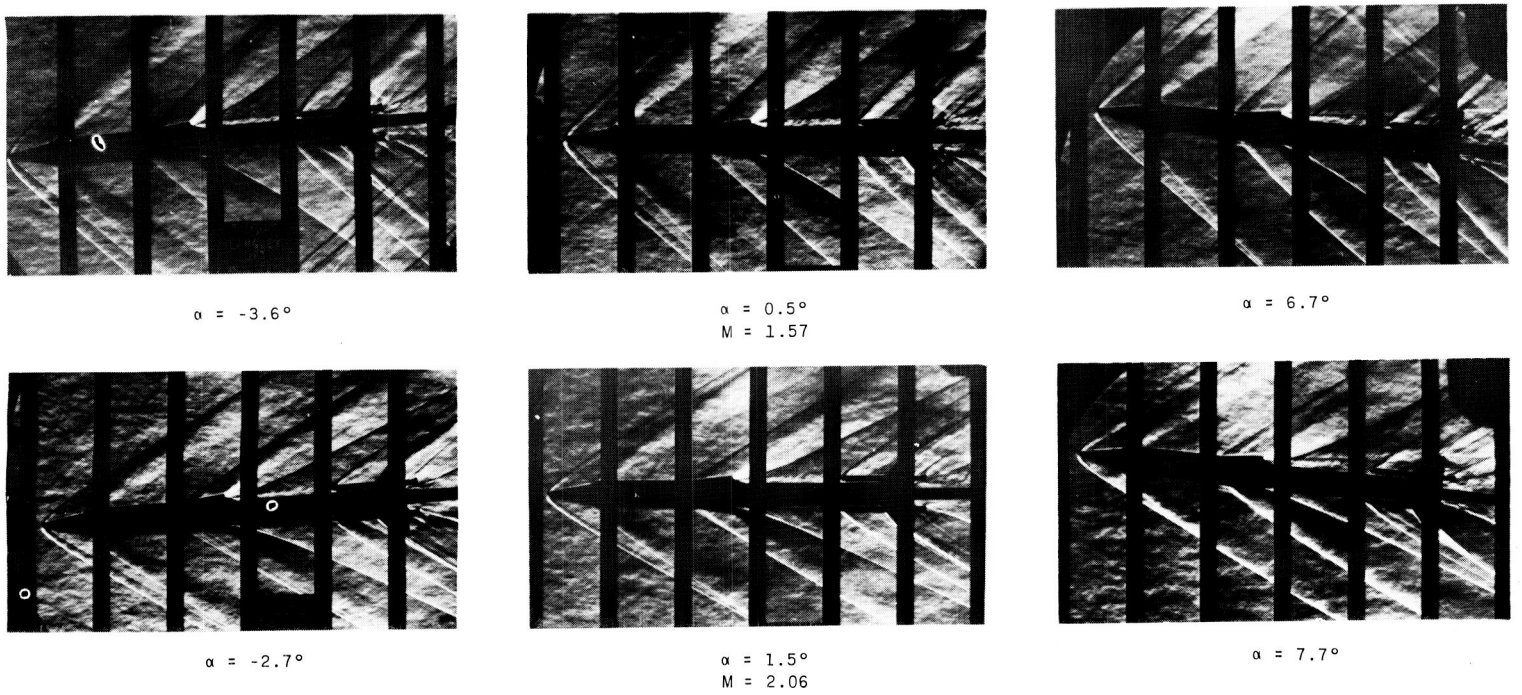

(b) $\phi = 90^{\circ}$.

L-59-6037

Figure 6.- Concluded.

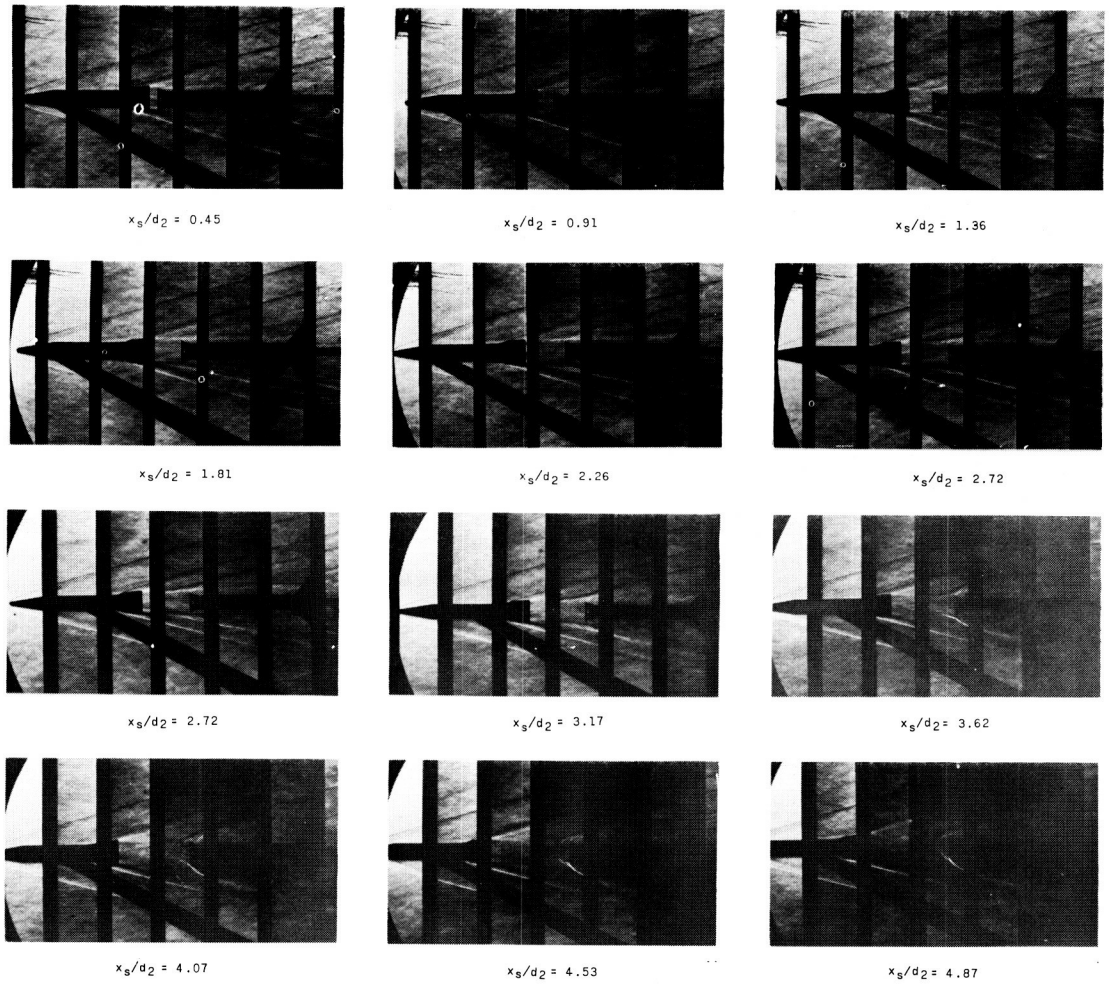

(a) $\alpha = 0.9^\circ$.

L-59-6038

Figure 7.- Schlieren photographs during separation. $M = 4.50$; $R = 1.6 \times 10^6$; $\phi = 0^\circ$.

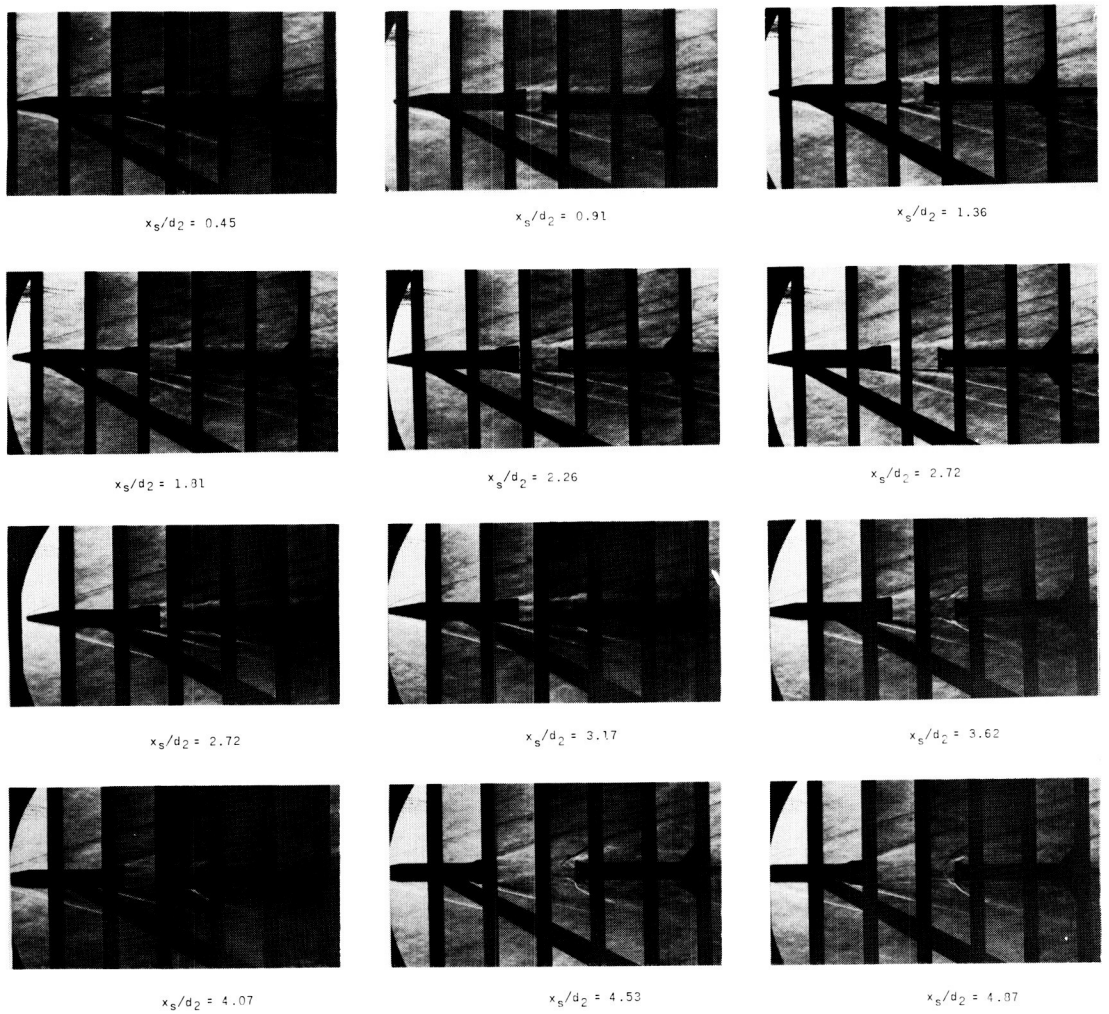

(b) $\alpha = 1.9^{\circ}$. L-59-6039

Figure 7.- Concluded.

α = -3.0°

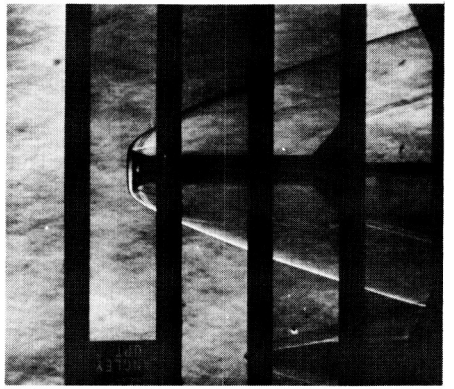

α = 0.9°

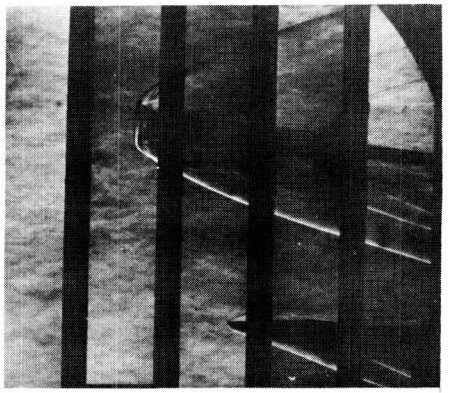

α = 7.0°

L-59-6040

Figure 8.- Schlieren photographs of stage I. M = 4.50; R = 1.6×10^6; $\phi = 0^\circ$.

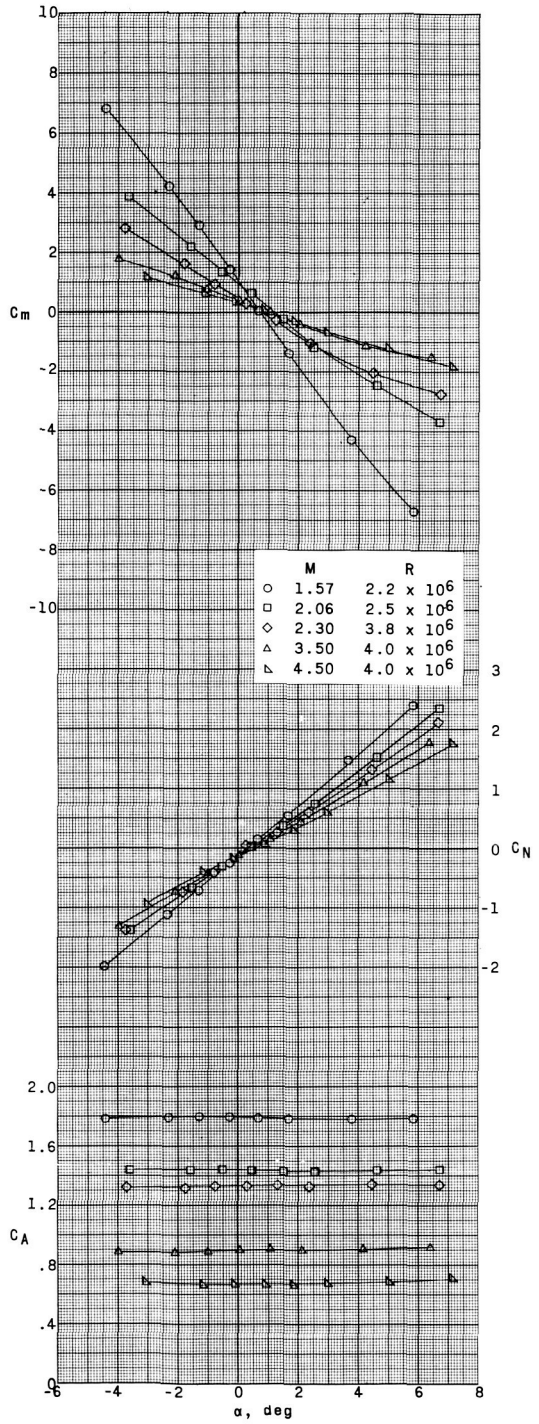

Figure 9.- Aerodynamic characteristics of the complete configuration in pitch. $\phi = 0^{o}$; small fins.

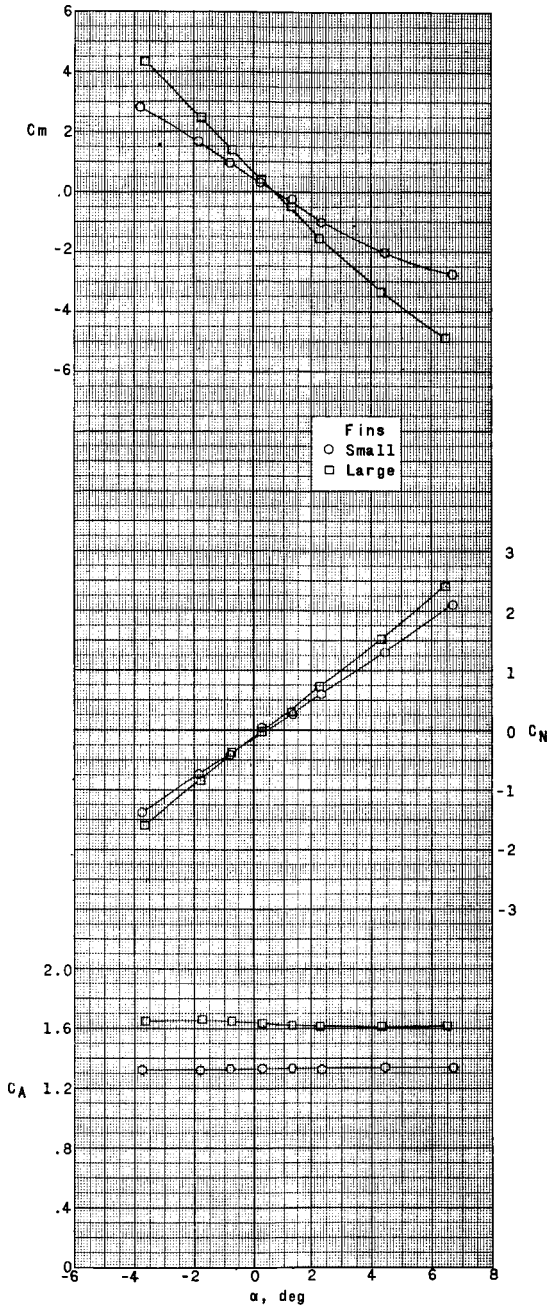

(a) M = 2.30.

Figure 10.- Effect of fin size on the aerodynamic characteristics of the complete configuration in pitch. $\phi = 0^{\circ}$.

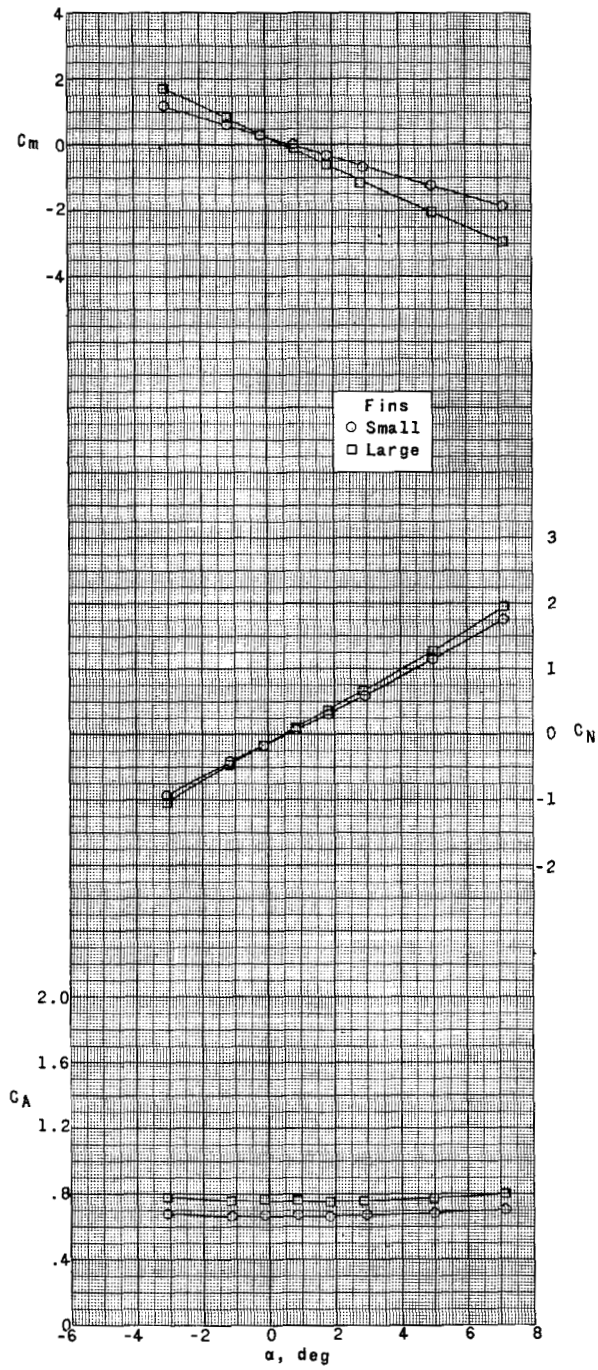

(b) M = 4.50.

Figure 10.- Concluded.

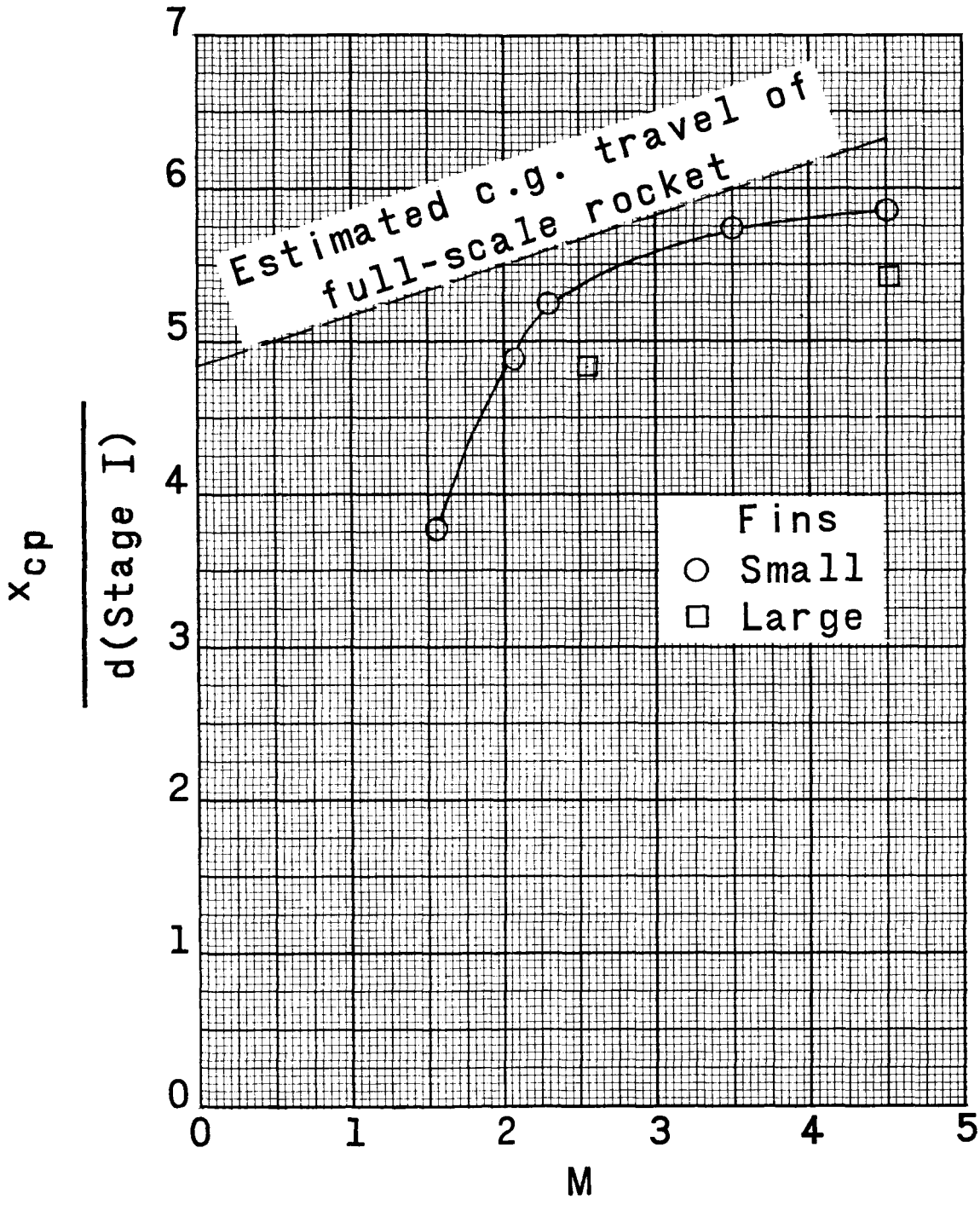

Figure 11.- Center-of-pressure variation with Mach number for the complete configuration.

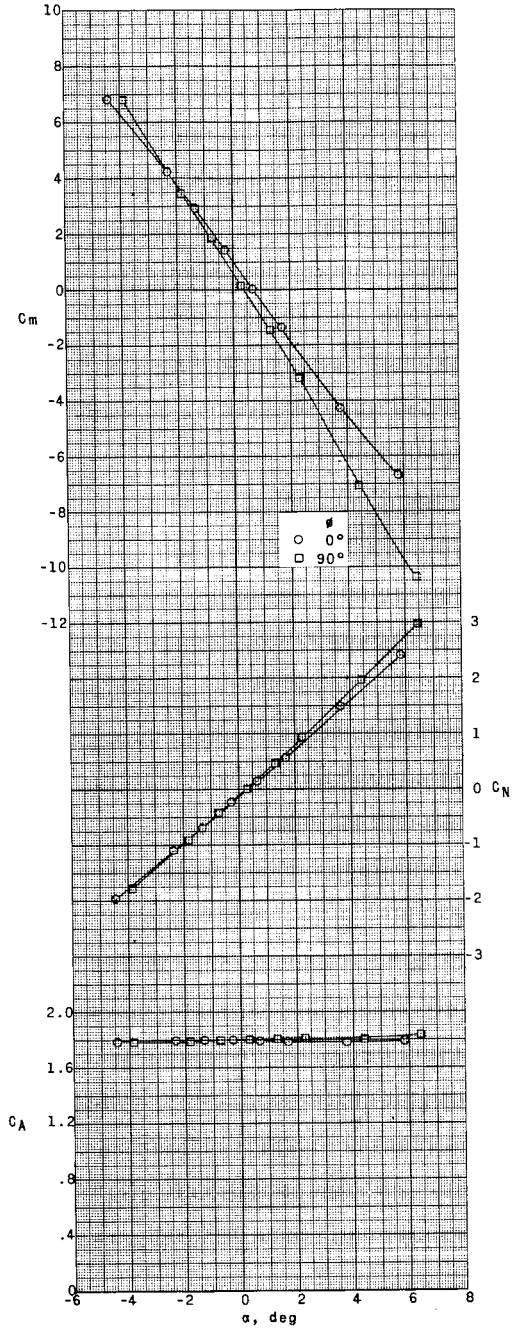

(a) M = 1.57; R = 1.6×10^6; small fins.

Figure 12.- Effect of model roll angle on the aerodynamic characteristics of the complete configuration in pitch.

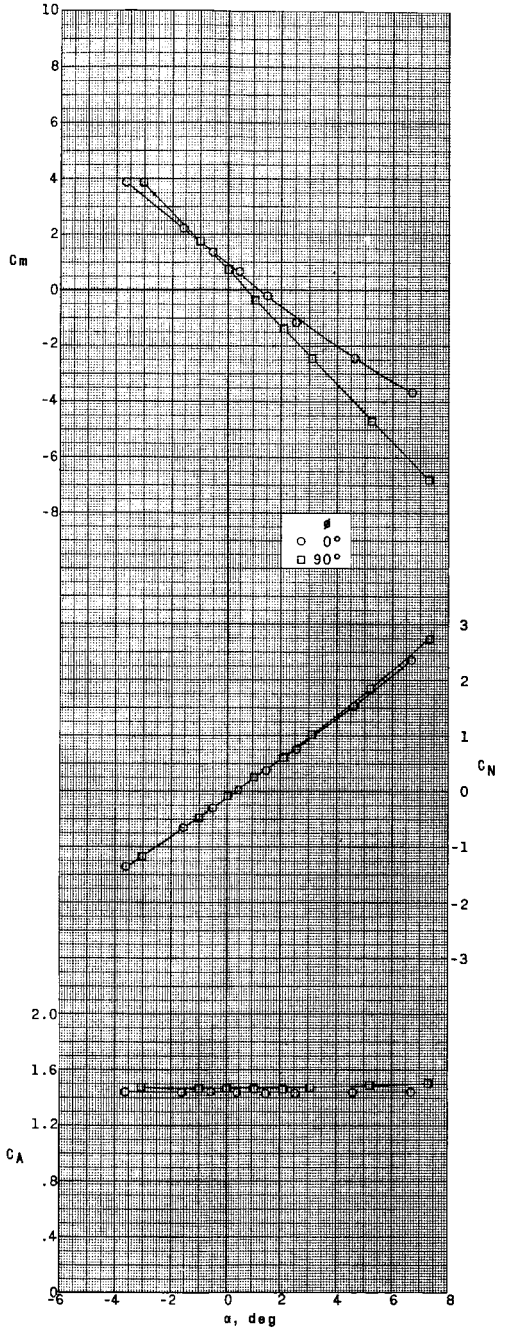

(b) M = 2.06; R = 2.1 × 10^6; small fins.

Figure 12.- Concluded.

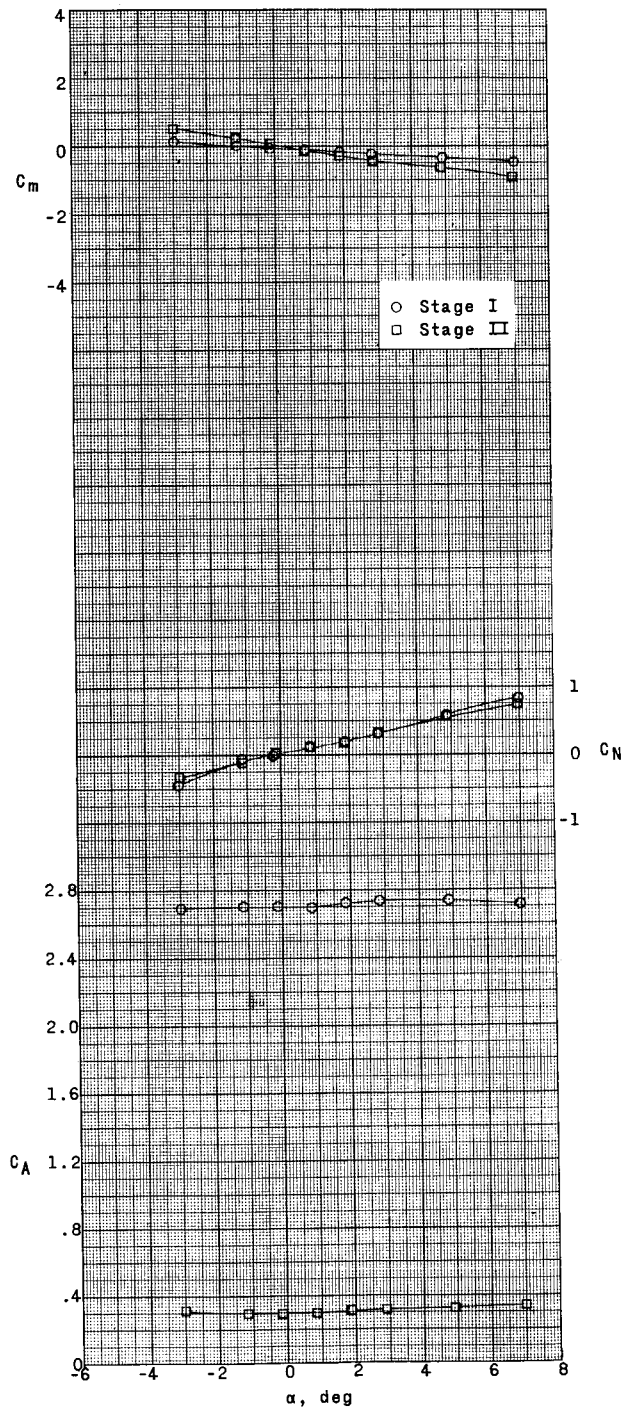

Figure 13.- Aerodynamic characteristics of stage I and stage II in pitch. $M = 4.50$; $R = 1.6 \times 10^6$; $\phi = 0^\circ$.

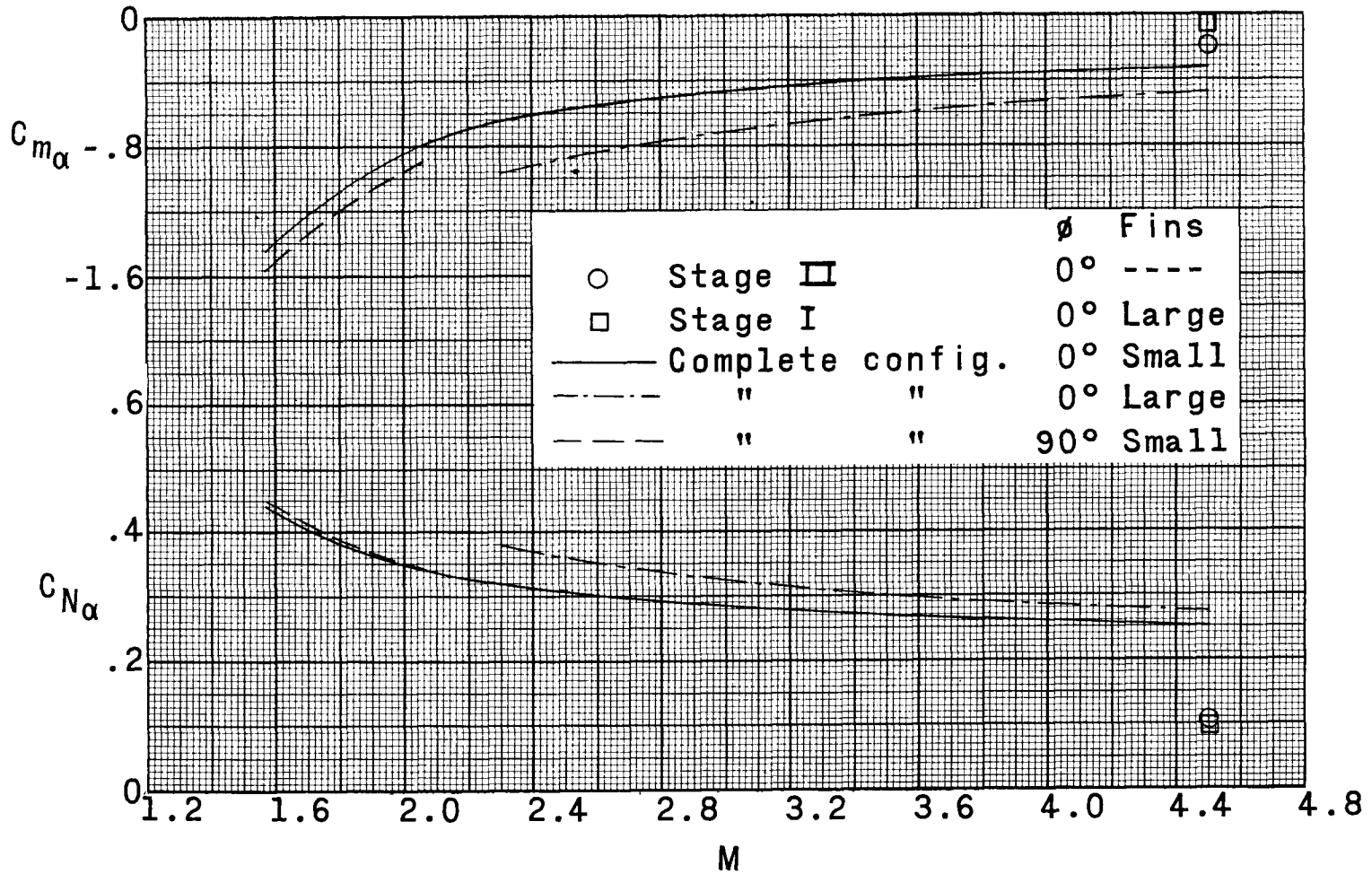

Figure 14.- Variation of stability characteristics with Mach number.

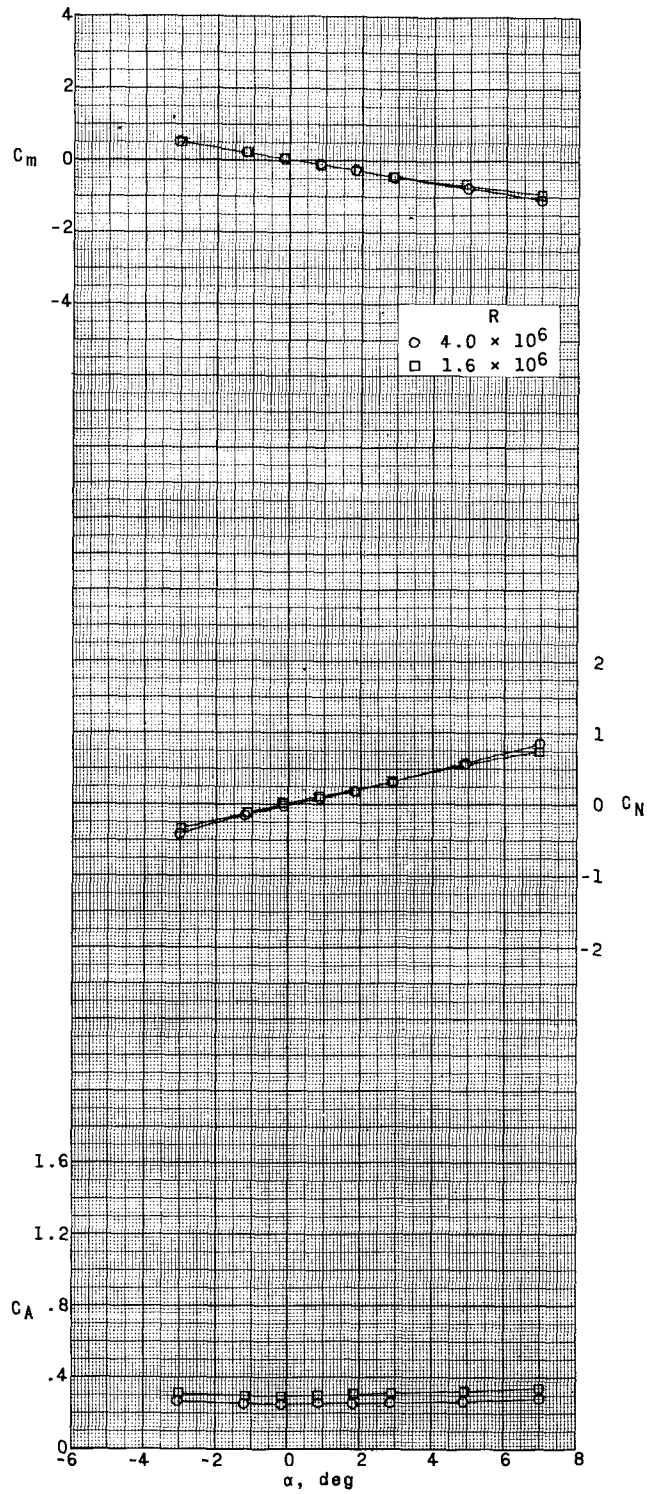

Figure 15.- Effect of variation in Reynolds number on the aerodynamic characteristics of stage II in pitch. M = 4.50; $\phi = 0^{o}$.

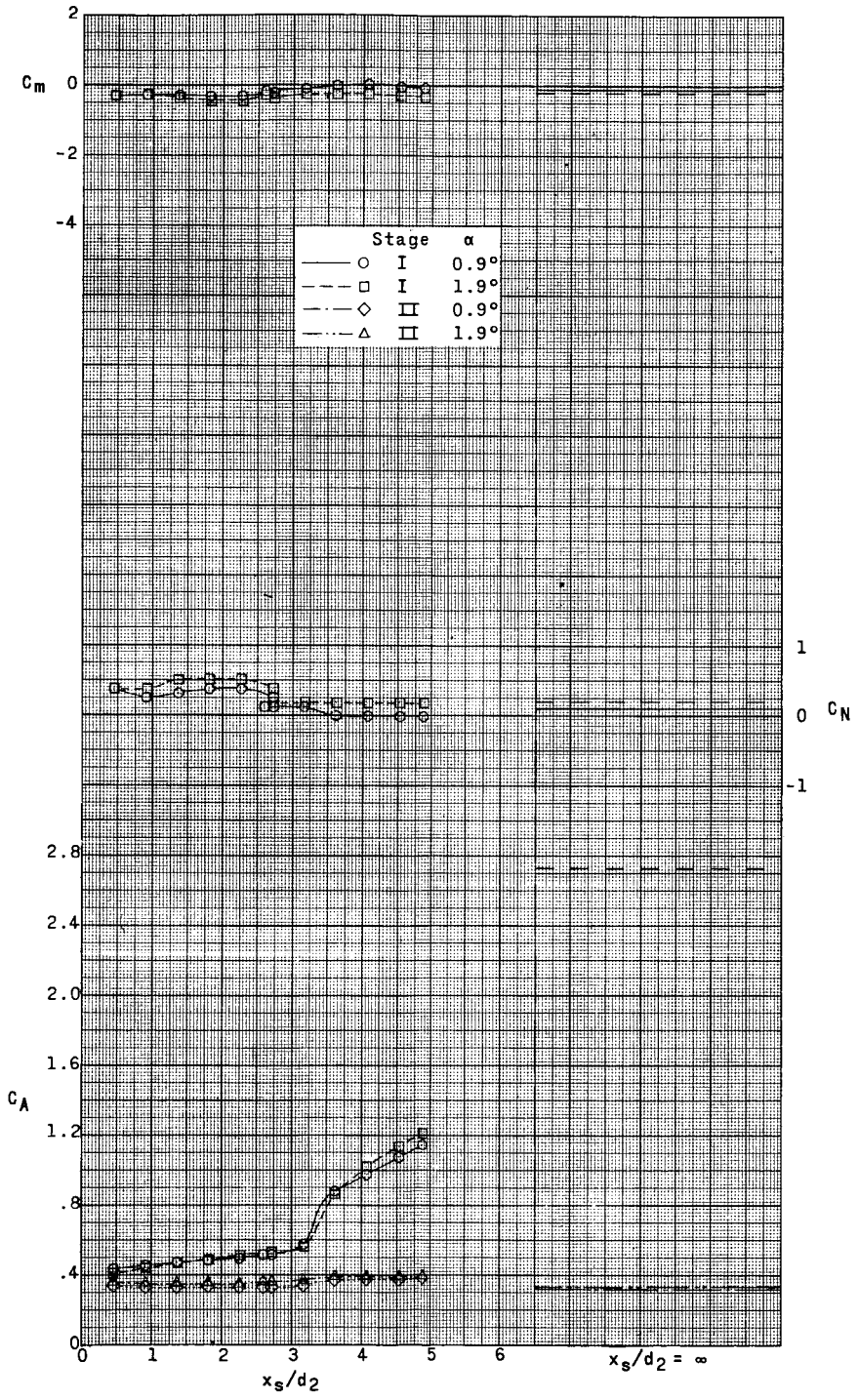

Figure 16.- Effect of separation on the aerodynamic characteristics of stage I and stage II. M = 4.50; R = 1.6×10^6; $\phi = 0^\circ$; small fins.

L-472